Dynamics of the IR-to-blue wavelength upconversion in Pr^{3+}-doped yttrium aluminum garnet and $LiYF_4$ crystals

M. Malinowski
Institute of Microelectronics and Optoelectronics, ul. Koszykowa 75, 00-662 Warsaw, Poland

M. F. Joubert and B. Jacquier
Laboratoire de Physico-Chimie des Materiaux Luminescents, URA 442 du CNRS, Universite Lyon 1, Bâtiment 205, 69622 Villeurbanne, France

(Received 18 February 1994)

The infrared-to-blue upconversion in Pr^{3+}-doped yttrium aluminum garnet and yttrium lithium fluoride crystals has been studied at temperatures between 4.4 and 300 K for different activator concentrations. The excitation spectra and decay-time measurements indicated the sequential absorption of two photons between levels of the $4f^2$ electronic configuration. The first photon is absorbed nonresonantly by a weak phonon band associated with the $^3H_4 \rightarrow {}^1G_4$ transition; the second resonant absorption step is from the $^1G_4(1)$ to one of the $^1I_6$ levels that relax to the $^3P_0$ state. Transitions from the excited $^1G_4$ state obeyed the spin and point symmetry selection rules for electric-dipole transitions. Excited-state-absorption spectra revealed structure not observed in one photon absorption and excitation spectra.

I. INTRODUCTION

The trivalent praseodymium (Pr^{3+}) ion is an attractive optical activator, since its energy-level spectrum contains several metastable multiplets $^1G_4$, $^1D_2$, $^3P_{0,1,2}$, that offer the possibility of simultaneous emission in the blue, green, orange, red, and infrared (IR).[1] Furthermore, the broadband interconfigurational $4f^2 \rightarrow 4f5d$ transitions of Pr^{3+} which are used in scintillator detectors of ionizing radiation[2,3] offer the potential for tunable laser action at near ultraviolet (UV) wavelengths. Up to now tunable UV stimulated emission has been observed only in Ce^{3+}-doped fluoride crystals.[4] Recently, Ganem, Dennis, and Yen[5] reported a sequential upconversion pumping process using blue light to achieve UV fluorescence in Pr^{3+}-doped yttrium aluminum garnet (YAG:Pr^{3+}), and Gayen, Xie, and Cheung measured two-photon (TP) transitions from the $^3H_4$ ground state to the $4f5d$ band in the same system.[6]

Recently, there has been a renewed interest in studying praseodymium doped materials for laser purposes, both continuous wave (cw) and pulsed, in crystals such as $YAlO_3$:Pr^{3+} (Ref. 7) and $LaCl_3$:Pr^{3+} (Ref. 8) as well as in optical fibers.[9] Blue laser operation at room temperature in $LiYF_4$:Pr^{3+} crystals has been reported by Esterowitz *et al.*,[10] and recently 487.9-nm laser emission has been observed at cryogenic temperatures in YAG:Pr^{3+}.[11] Smart *et al.*[12] reported on Pr^{3+}-doped fluorozirconate fiber lasers that were pumped at two infrared wavelengths (835 nm and 1.01 μm) and lased at five visible wavelengths at room temperature. Allain, Monerie, and Poignant[13] observed room-temperature upconversion lasing in a Yb:Pr codoped fluoride fiber pumped by one Ti:sapphire laser in the 810–870-nm phonon sideband of the Yb^{3+} absorption.

The possibility of realizing an upconversion laser pumped at infrared wavelengths where high power GaAlAs laser diodes are available, has renewed our interest in the study of excitation mechanisms in YAG:Pr^{3+} and $YLiF_4$:Pr^{3+} (YLF:Pr^{3+}) crystals. In upconversion laser schemes, excitation of high-energy optical states is achieved either by sequential absorption of pump photons in one ion, or by cooperative transfers involving two or more excited ions or as shown recently, by photon avalanche, i.e., a process that involves cross relaxation to populate the metastable states of two ions followed by excited-state absorption (ESA) from these states.[14]

While most upconversion studies in Pr^{3+}-doped materials have focused on the $^1D_2 \rightarrow {}^3P_0$ processes,[15,16] the alternate $^1G_4 \rightarrow {}^1D_2$, $^3P_0$ process was only observed in Pr^{3+} fibers[12,13] and has not been well characterized. The present spectroscopic studies focus on upconversion excitation of higher-lying states of Pr^{3+}-doped YAG and YLF crystals by near-IR excitation of the $^1G_4$ state. This type of excitation also provides a useful tool to access high-energy levels not easily explored by other spectroscopic techniques and allows one to study the levels of the $^1I_6$ manifold for which transitions from the ground state are spin forbidden. The high-energy levels of Pr^{3+} in these crystals have not been well documented and there are still ambiguities regarding the $^1I_6$ and ^3P_J energy-level assignments. Experimental values for YAG:Pr^{3+}, obtained by means of one-photon (OP) absorption and excitation spectroscopy, were given by Antic-Fidancev *et al.*[17] Calculated, theoretical values were reported by Gruber *et al.*[18] and Esterowitz *et al.*[10] for Pr^{3+}-doped YAG and YLF, respectively. The present work suggests the potential for IR upconversion pumped lasing in Pr^{3+}-doped YAG and YLF.

0163-1829/94/50(17)/12367(8)/$06.00

The experimental apparatus is described in Sec. II and experimental results on upconversion in YAG:Pr^{3+} and YLF:Pr^{3+} are described in Secs. III A and III B, respectively. In Sec. IV the results of Sec. III are compared to the OP data and analyzed and discussed in the framework of a proposed upconversion model. Finally some conclusions are drawn in Sec. V.

II. EXPERIMENTAL METHODS

Several YAG:Pr^{3+} samples with concentrations 0.08, 0.24, and 0.6 at. % as determined by x-ray-fluorescence analysis were grown parallel to the ⟨111⟩ direction using the Czochralski technique at ITME Laboratory in Warsaw. The $LiYF_4$:0.24 at. % Pr^{3+} crystal was obtained from the Lawrence Livermore National Laboratory.

The YAG sample has a cubic space-group symmetry O_h^{10}. The Pr^{3+} ions substitute for Y^{3+} ions on the dodecahedral sites having D_2 symmetry.[18] The YLF sample has the sheelite structure with space group C_{4h}^6. The Pr^{3+} ions substitute for Y^{3+} ions in S_4 symmetry sites.[20]

Absorption measurements in the range from 195 to 1050 nm, were made using a Cary 2300 Varian spectrometer equipped with a continuous-flow helium cryostat. Fluorescence and excitation spectra were obtained using a tunable dye laser operated with Rhodamine 590 and Coumarine 480 pumped by a frequency doubled or tripled Quantel Model 481 Nd:YAG laser (10-ns pulse length, 10-Hz repetition rate, and 350-mJ energy per pulse at 532 nm). For excitation in the IR region the output wavelength of a tunable laser operated with DCM dye was downshifted by 4155 cm^{-1} by stimulated Raman scattering in a high-pressure gaseous H_2 cell. A continuous wave (cw) excitation in the IR region was achieved with a Coherent Radiation Model 899-1 Ti^{3+}:sapphire laser pumped by an Innova 310, 10-W argon ion laser. The spectra were recorded using a Hilger and Watts 1-m monochromator with dispersion of 8 Å/mm and detected by an S-20 EMI 9789 or a cooled GaAs RCA C31034-02 photomultiplier. For infrared detection, a highly sensitive Model 403L cooled germanium photodetector from Applied Detector Corporation was used. Data acquisition was with an Ortec photon counting system controlled by a personal computer. Fluorescence lifetime measurements were performed with a Stanford Research SR430 multichannel analyzer. Sample cooling was provided by a liquid-He optical cryostat with a gas heating system that allowed varying the temperature between 1.6 and 300 K.

Since the transition linewidths in YAG:Pr^{3+} strongly depend on activator concentration, and additional spectra from Pr^{3+} ions occupying several perturbed sites have been reported,[17,19] our energy-level assignments were based on measurements in a diluted 0.08% Pr^{3+}-doped sample.

III. RESULTS

A. YAG:Pr^{3+}

We have observed blue upconverted emission for several excitation wavelengths around 11 100 cm^{-1} (900 nm) over the temperature range from 4.4 to 300 K. Figure 1 shows the upconverted emission spectrum of the YAG:0.6% Pr^{3+} sample under pulsed IR excitation at 11 039 cm^{-1} (905.9 nm). The light intensity at the sample was about 260 MW/cm^2. Two emission lines at 486.9 and 487.9 nm were ascribed to the $^3P_0 \rightarrow {}^3H_4(1,3)$ transitions. Emission from the $^3P_0$ level, which has Γ_1 symmetry, to the first excited $^3H_4(2)$ Stark level at 19 cm^{-1} also having Γ_1 symmetry is forbidden by the symmetry selection rules[16] and was not observed in the spectrum of Fig. 1. The excitation spectra of the $^3P_0$ emission at 486.9 nm, after pulsed and cw IR excitations, are presented in Fig. 2. The cw pumping had an intensity of 0.14 kW/cm^2

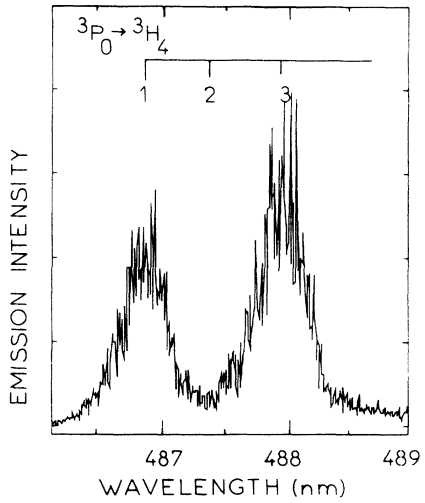

FIG. 1. Upconversion fluorescence spectrum in YAG:0.6% Pr^{3+} resulting from IR, 11 039 cm^{-1} (905.9 nm) pumping, $T=4.4$ K.

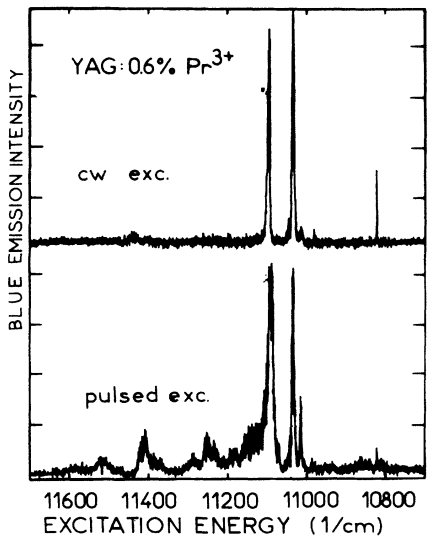

FIG. 2. Excitation spectra of the $^3P_0$ (486.9 nm) emission in YAG:0.6% Pr^{3+} obtained at 4.4 K after pulsed and cw IR pumping.

at the sample. The spectra consist of four narrow lines at 11 096, 11 039, 11 019, and 10 826 cm^{-1} (901.2, 905.9, 907.5, and 923.7 nm, respectively) and several less intense, broader transitions, more pronounced in the case of pulsed excitation, on the short-wavelength side.

In order to determine the mechanism of the upconversion process, the lifetime of the $^3P_0$ state and the dependence of the emission intensity versus IR excitation energy have been measured. Figure 3 shows the 4.4-K decay profiles of the $^3P_0$ level at 486.9 nm in 0.08% and 0.6% Pr^{3+}-doped samples following IR excitation at 11 039 cm^{-1}. For all investigated Pr^{3+} concentrations the $^3P_0$ state exhibited an exponential decay with the low-temperature lifetime of 13 μs. This behavior is typical of an ESA process and is confirmed by direct excitation into the $^3P_0$ level. Indeed, Fig. 3 also shows the 4.4-K decay profile of the $^3P_0$ level, measured by monitoring $^3P_0 \rightarrow {}^3F_2$ fluorescence at 620 nm, under direct excitation

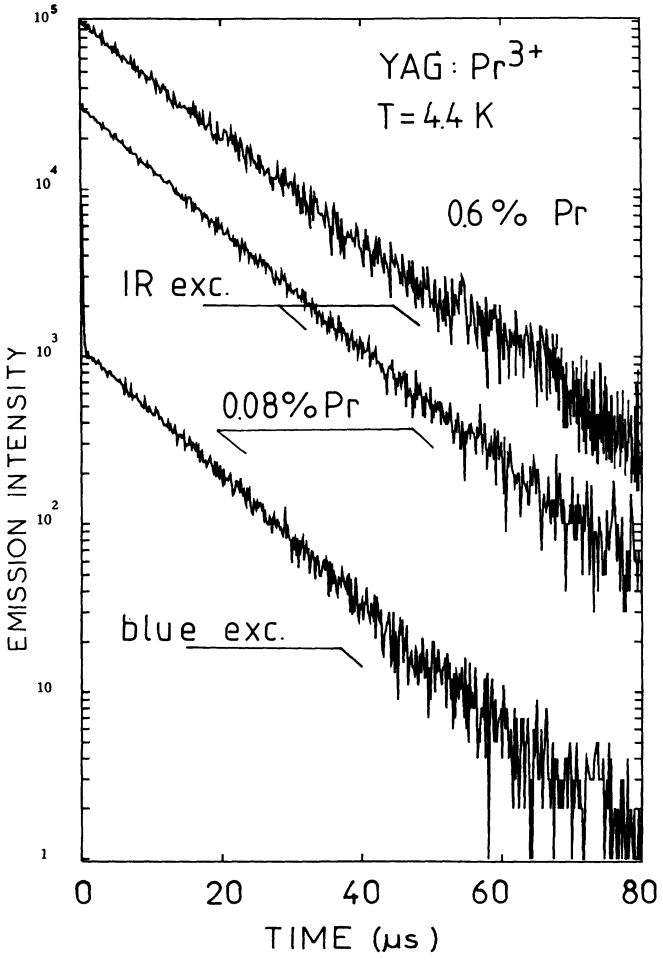

FIG. 3. Decay profiles of the upconverted $^3P_0 \rightarrow {}^3H_4$ (486.9 nm) luminescence in YAG:Pr^{3+} resulting from the IR 11 039 cm^{-1} (905.9 nm) pumping, the lower trace shows the decay profiles of the $^3P_0 \rightarrow {}^3F_2$ (620 nm) luminescence after direct, blue excitation at 20 538 cm^{-1} (486.9 nm) in YAG:0.08% Pr^{3+}, T=4.4 K.

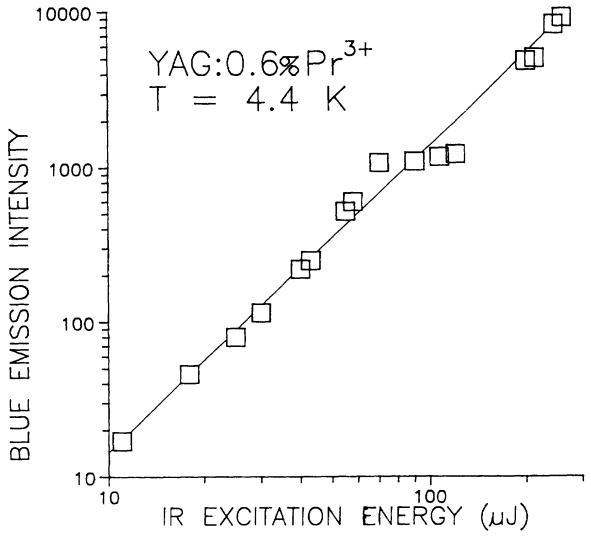

FIG. 4. Variation of the upconverted $^3P_0$ (486.9 nm) luminescence with the IR excitation intensity at 11 039 cm^{-1} (905.9 nm) in YAG:Pr^{3+}. The solid curve illustrates a square dependence.

at 20 538 cm^{-1} (486.9 nm). Directly excited $^3P_0$ decay curves for Pr^{3+} concentrations of 0.08 (see Fig. 3), 0.24, and 0.6% (not presented) exhibited an almost exponential decay. The long-time decay in the 0.08% Pr^{3+}-doped sample indicated an isolated ion lifetime τ_0 of 13.5 μs. Furthermore, the upconversion fluorescence intensity from the $^3P_0$ level increases as the square of incident pump power, as shown in Fig. 4. It should be noted a fast (less than 0.5 μs) component observed for direct excitation which will be discussed in the next part.

IR excitation also resulted in much slower decay, with a lifetime of 245 μs in 0.08% Pr^{3+}-doped sample. The emission at 610 nm from the $^1D_2$ state exhibited a rise time of 9 μs as shown in Fig. 5.

B. $LiYF_4$:Pr^{3+}

Blue upconverted emission has also been observed in a praseodymium-doped $LiYF_4$ (YLF) crystal after pulsed IR excitation with a 260-MW/cm^2 intensity at the sample. The low-temperature σ-polarized IR excitation spectrum of the $^3P_0$ emission at 479.5 nm is presented in Fig. 6. It consists of two strong lines at 11 775 and 11 714 cm^{-1} (849.2 and 853.7 nm, respectively) and some less intense features observed on the long-wavelength side of the spectrum. The π-polarized spectrum revealed one strong transition at 11 542 cm^{-1} (866.4 nm). Decay curves of the $^3P_0$ level measured at 4.4 K after IR and direct blue excitation are presented in Fig. 7. For both excitation schemes, the decay was exponential with a lifetime of 52 μs. Slow decay in the orange part of the spectrum was observed neither after IR nor direct excitation of the $^3P_0$ level. As for YAG:Pr^{3+} a square law intensity dependence of the upconverted $^3P_0$ fluorescence was determined.

IV. DISCUSSION

It was seen that IR excitation resulted in a $^3P_0$ decay with no observable rise time and with a long-time decay that did not change with respect to that for direct excitation of $^3P_0$. This, together with the quadratic intensity dependence of the blue emission on the incident IR photon flux, indicates a sequential two-photon absorption process. However, in the case of YAG:Pr^{3+}, the structure observed in Fig. 2 after intense pulsed excitation could be due to direct two-photon absorption (TPA) $^3H_4(\Gamma_3) \rightarrow {}^3P_2(\Gamma_i)$ transitions which are all allowed in D_2 symmetry.[21] According to the $^3P_2$ levels reported in Ref. 18, the photon energies for TPA transitions to the $^3P_2$ Stark levels lie in the 11 052--11 208 cm^{-1} band and TPA may overlap with the ESA transitions. This could also explain the absence of structure in the upper spectrum of Fig. 2 for the case of less intense cw excitation. For YLF:Pr^{3+} TPA could be ruled out because the half values of the $^3P_2$ energies[10] lie below the spectral region investigated here and shown in Fig. 6.

The initial fast $^3P_0$ decay measured in YAG:Pr^{3+} under direct OP blue excitation shown in Fig. 3, could be explained by the overlapping of the $^3P_0$ fluorescence with the broadband upconverted emission originating from the $4f5d$ band[5,6] and terminating at the $^1D_2$ manifold. This is also confirmed by our lifetime measurements of a similar fast fluorescence decay at wavelength nonresonant with the $^3P_0$ emission.

The only possible (ESA) mechanism resulting in the excitation of the $^3P_0$ state with IR photons should come from the excited $^1G_4$ state. In that case, the IR pump wavelength must be resonant only with the absorption from the intermediate metastable $^1G_4$ state to $^3P_{0,1}$ or $^1I_6$ states, but not with the absorption from the ground $^3H_4$ state. Thus the first photon is nonresonantly absorbed in a weak phonon band associated with the $^3H_4 \rightarrow {}^1G_4$ transition. Figure 8 shows a relevant part of the Pr^{3+}

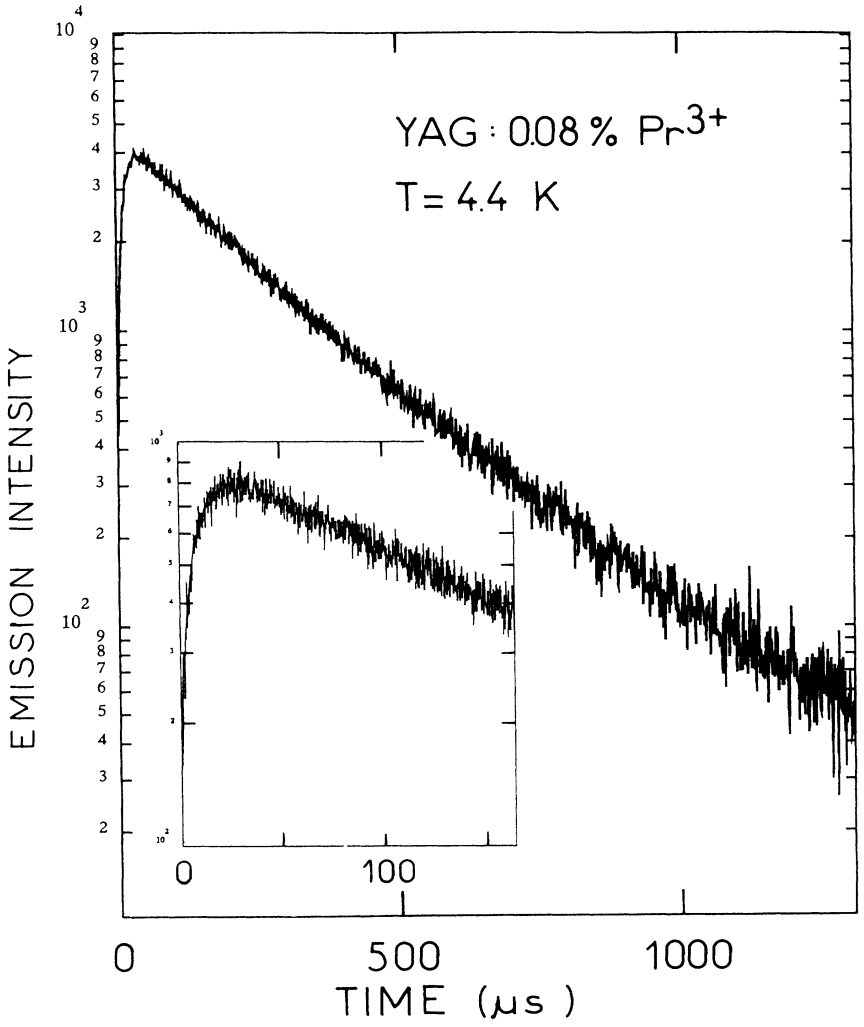

FIG. 5. Decay profile of the $^1D_2$ emission, following IR upconversion excitation of the $^3P_0$ state at 4.4 K.

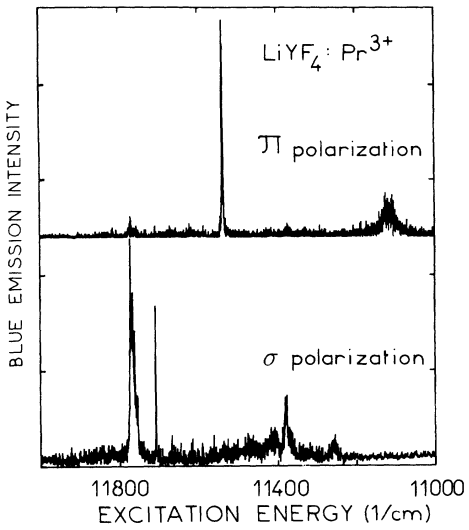

FIG. 6. Polarized excitation spectra of blue emission at 479.5 nm in YLF:Pr^{3+}, $T=4.4$ K.

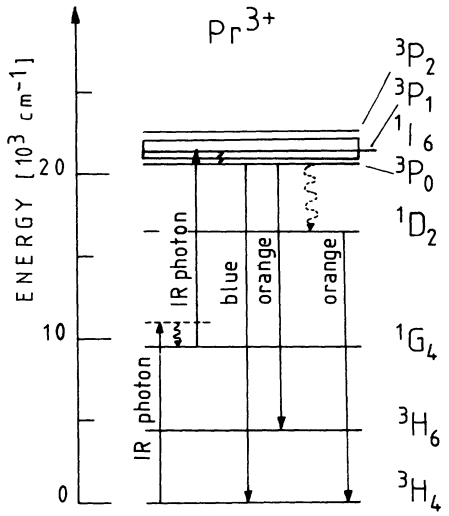

FIG. 8. Simplified energy-level diagram for Pr^{3+} ion showing upconversion excitation and emission transitions.

energy-level diagram, and the proposed excitation scheme.

The IR low-temperature absorption ($^3H_4 \rightarrow {}^1G_4$ transition) and excitation spectra of the $^1G_4 \rightarrow {}^3H_5$ emission at 1.3 μm were also measured. These allowed us to determine the position of the Stark levels of the $^1G_4$ multiplet and to identify the lowest crystal-field level of the $^1G_4$ manifold at 9712 and 9699 cm^{-1}, respectively in Pr^{3+}-doped YAG and YLF. These values are in good agreement with the reported experimental data on these crystals.[10,18,20]

We made a special effort to study the high-energy Pr^{3+}

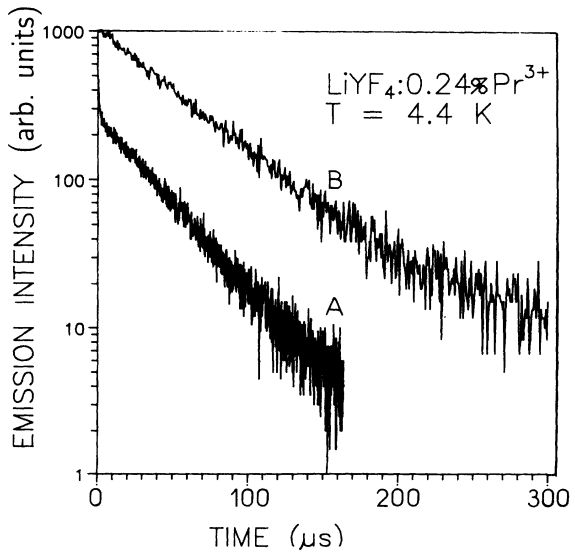

FIG. 7. Decay curves of the $^3P_0$ level in YLF:Pr^{3+} after; (a) direct blue excitation at 21 477 cm^{-1}, (b) upconversion IR pumping at 11 778 cm^{-1}, $T=4.4$ K.

TABLE I. Energy-level position of the $^1G_4$, $^1I_6$, and $^3P_{0,1}$ manifolds in YAG:Pr^{3+} (point group D_2) and $LiYF_4$:Pr^{3+} (point group S_4) determined in this work. Polarization identification refers to the ground-state transitions.

	YAG:Pr^{3+}		$LiYF_4$:Pr^{3+}		
Manifold	E (cm^{-1})	Γ	E (cm^{-1})	Γ	pol.
$^3P_1$	21 142	4	21 494	1	π
	21 045	2			
	21 030		21 416	3,4	σ
$^1I_6$	21 875	2	21 772	1	π
	21 830[a]	4			
	21 676	4			
	21 641	1			
	21 236[a]	3	21 477	3,4	σ
	21 172	3	21 470[a]		
	21 135[a]	2	21 241	2	π
	21 123	1			
	21 055	1			
	20 855	2			
	20 809	4	21 082	3,4	σ
	20 751	3	21 011[a]		
	20 732	1			
$^3P_0$	20 538	1	20 866	1	π
$^1D_2$	17 210	4	17 406	2	
	17 088	3	17 083	3,4	σ
	16 881	1	16 810	1	π
	16 408	2	16 740	2	
	16 399	1			
$^1G_4$	10 284	2	10 474	1	π
	10 261		10 426		
	10 127		10 313		
	10 114	4	10 129		σ
	9 852		10 113		π
	9 833		9 910[a]	2	
	9 823	1	9 831	3,4	σ
	9 712	2	9 699	1	π
$^3H_4$	0	3	0	2	

[a]Denotes less accurate results.

levels, that participate in the second step of the proposed ESA process. Precise OP excitation and absorption measurements at 4.4 and 130 K have been performed. They confirmed some of the earlier assignments of the $^3P_{0,1}$ levels[10,18] and allowed us to assign positions to certain of the $^1I_6$ levels listed in Table I. To resolve the overlapping of several lines in YAG:Pr^{3+}, the concentration dependence of the relative intensities of the $^3H_4 \rightarrow {}^3P_0$ and $^3H_4 \rightarrow {}^1I_6$ transitions, reported earlier by Galczynski, Blazej, and Strek[22] for LaF_3:Pr^{3+} was examined as shown in Fig. 9. For YLF:Pr^{3+} the π-polarized absorption spectrum indicated $^3P_0$ singlet at 20 866 cm^{-1}. For both polarizations, the excitation spectra revealed an intense vibronic structure, also observed by Donegà, Meijerink, and Blasse,[23] on the high-energy side of the $^3P_0$ level, making any assignment in this energy band impossible. Several strong polarized transitions were observed at 21 416, 21 477, 21 494, and 21 772 cm^{-1}.

The next step in our analysis was to compare these OP spectra with the ESA spectra of the $^3P_0$ blue emission. The spectra from Figs. 2 and 6 were replotted taking as the origin of wavelength axis the position of the lowest lying $^1G_4$ Stark level, and they are presented together with OP data in Figs. 10 and 11. The final energy-level assignments in YAG and YLF were made by taking into account the different selection rules for OP and ESA transitions due to different Γ for the lowest components of $^3H_4$ and $^1G_4$ levels.

In the case of YAG, important differences between the OP absorption and ESA spectra could be observed. Detailed examination revealed that the structure seen in ESA spectra of YAG:Pr^{3+} resulted mostly from $^1G_4(1) \rightarrow {}^1I_6$ transitions. In the ESA spectrum from Fig. 10 the weak line at 20 538 cm^{-1} corresponded to the $^1G_4 \rightarrow {}^3P_0$ transition, and transitions to the $^3P_1$ Stark levels were not observed. In particular, there was no ground-state transition to the $^1I_6$ level at 20 751 cm^{-1} where the strong ESA transition at 11 093 cm^{-1} (905.9 nm) terminates, suggesting that the $^1I_6$ level has a Γ_3 symmetry. The absence of a transition to the 20 836 cm^{-1} level in the ESA spectrum is an indication of its Γ_2 symmetry as its origin at the lowest $^1G_4$ level is also Γ_3.

In the YLF crystal, the strong σ-polarized line at 21 477 cm^{-1} and the π-polarized line at 21 241 cm^{-1} shown in Fig. 11 were due to ESA up to the $^1I_6$ level. Relatively less intense than in the OP spectrum, the transition to the $^3P_1$ state at 21 335 cm^{-1} was also seen. At 4.4 K the transition from the excited $^1G_4(1)$ level to the $^3P_0$ level in YLF:Pr^{3+} was not observed. This was explained by the point-symmetry selection rules which forbid transitions between two levels of Γ_1 symmetry and was also confirmed by the observation at higher temperature of the σ-polarized lines assigned to transitions from the second $^1G_4(2)$ Stark level at 9832 cm^{-1} to the $^3P_0$ level as shown in Fig. 12. The π-polarized lines observed in Fig. 12 are due to $^1G_4(2) \rightarrow {}^1I_6$ transitions. The posi-

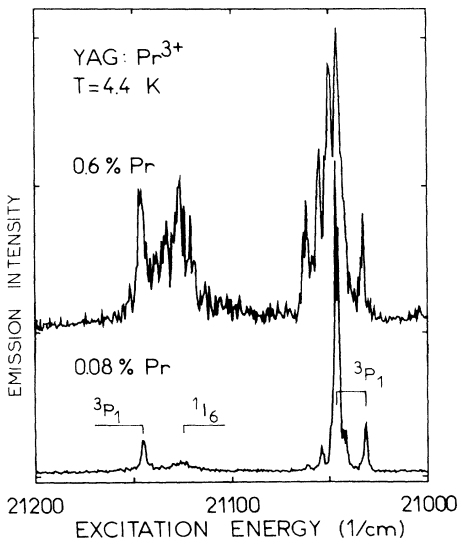

FIG. 9. One photon excitation spectra of the blue, 479.5-nm emission in; (a) 0.6% Pr^{3+}-, and (b) 0.08% Pr^{3+}-doped YAG, $T=4.4$ K. Note the change in the relative line intensities with concentration.

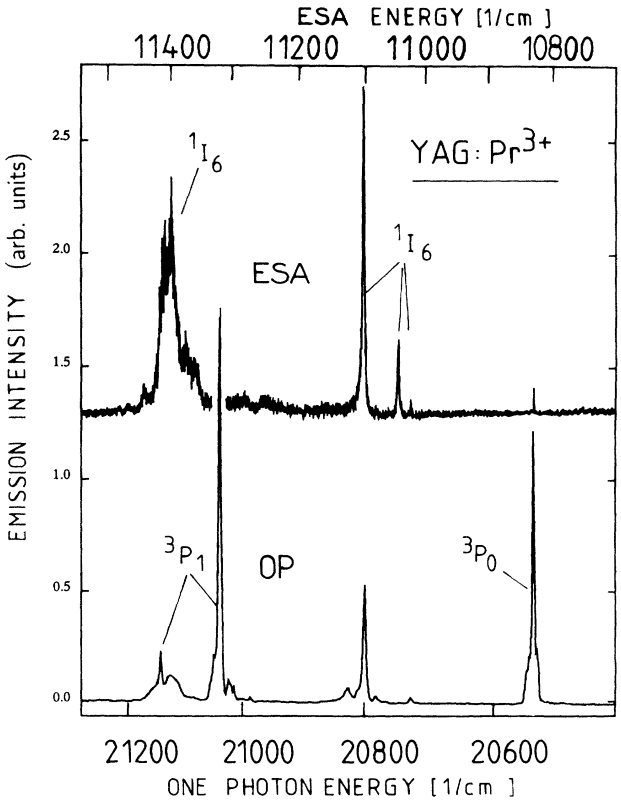

FIG. 10. Comparison of one photon (OP) and excited-state absorption (ESA) excitation spectra of the $^3P_0$ emission in YAG:0.08 Pr^{3+}. The origin of ESA excitation energy is the lowest Stark level, at 9712 cm^{-1}, in the $^1G_4$ manifold, $T=4.4$ K.

tion of the $^1G_4(\Gamma_2)$ level at 9910 cm^{-1}, to which transitions from the ground state (GSA) are forbidden, was determined from the 170 K ESA transition to the $^1I_6$ level at 21 772 cm^{-1}.

A summary of our energy-level assignments for Pr^{3+}-doped YAG and YLF is presented in Table I. It is seen

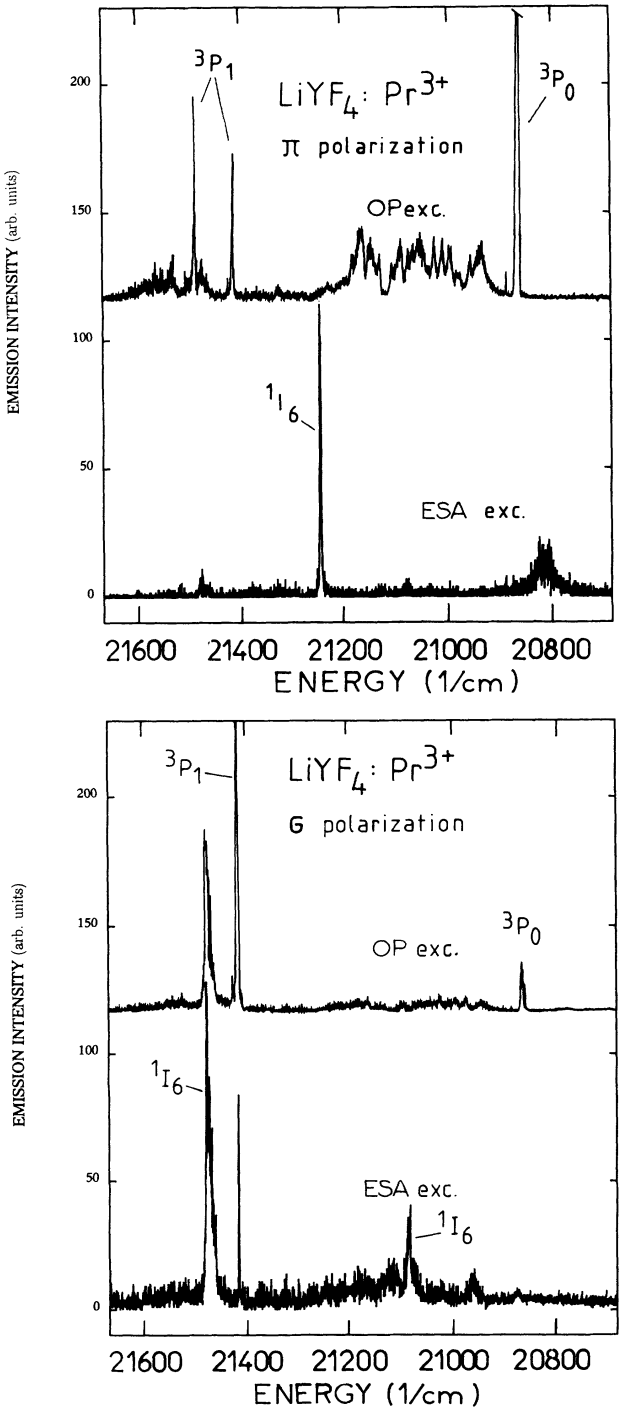

FIG. 11. Comparison of one-photon (OP) and excited-state absorption (ESA), polarized excitation spectra of the $^3P_0$ emission in YLF:Pr^{3+}. The origin of ESA excitation energy is the lowest Stark level, at 9699 cm^{-1}, in the $^1G_4$ manifold.

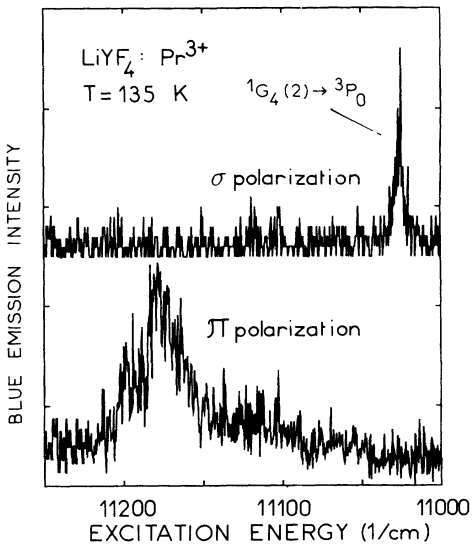

FIG. 12. Polarized IR excitation spectra of the $^3P_0$ emission in YLF:Pr^{3+} measured at 135 K showing thermally induced transitions from the second excited Stark level of the $^1G_4$ manifold.

that some of our measured Pr^{3+} energy values in YAG are in reasonable agreement with the 77-K data of Hooge[24] and Antic-Fidancev *et al.*;[17] however, we have extended their assignments. In the case of YLF:Pr^{3+}, two components of the $^3P_1$ manifold and several $^1I_6$ Stark components have been identified. It is known that in Pr^{3+} compounds the $^1G_4 \rightarrow {}^1I_6$ ESA transition is more than one order of magnitude stronger than the 1-μm $^3H_4 \rightarrow {}^1G_4$ GSA.[25] From the Judd-Ofelt parameters determined previously for YAG:Pr^{3+},[26] the ESA oscillator strength was found to be $f_{ESA} = 61 \times 10^{-6}$, which is about one hundred times the $f_{GSA} = 0.6 \times 10^{-6}$. In the case considered, the first step is nonresonant, into the phonon band above the $^1G_4$ multiplet, thus the overall efficiency of the IR-to-blue light conversion is strongly dependent on that. It was observed that under the same excitation conditions, sample sizes and doping levels (0.24 at. % Pr^{3+}), the $^3P_0$ fluorescence signal in YAG was more than one order of magnitude stronger than in YLF. As a consequence of multiphonon absorption to fill the $^1G_4$ level, it requires high phonon energies which are more probable in YAG (Ref. 27) than in YLF.[23] Furthermore, the energy gap between the $^1G_4$ and the $^3P_0$ is slightly less for YAG than for YLF. Both considerations agree that the experimental evidence of an ESA is more efficient in YAG than in YLF.

Another important factor in the upconversion process investigated here is the lifetime of the $^1G_4$ level. This was measured under direct IR excitation (988 nm) of the $^1G_4 \rightarrow {}^3H_5$ emission at 1.3 μm.[29] In the YLF:0.24% Pr^{3+} crystal the 4.4-K decay was nearly exponential and was temperature independent with a lifetime of 17 μs. In YAG:0.08% Pr^{3+} the decay was too fast to be followed by our Ge photodetector and could be estimated to be of the order of 0.4 μs. This large difference in the fluores-

cence lifetime was also explained by the difference in the effective phonon energies for nonradiative decay in YAG and YLF which are 865 and 566 cm^{-1}, respectively;[27,28] three and four phonons are needed, respectively, in YAG and in YLF, to bridge the energy gap of about 2200 cm^{-1} between $^1G_4$ and $^3F_4$ multiplets. The nonexponential behavior of the $^1G_4$ decay may be due to energy transfer since the concentration (0.24%) is high enough as we have noted earlier.[29]

The higher nonradiative transition probability in YAG was also responsible for the presence of the orange $^1D_2$ emission after $^3P_0$ excitation. The $^1D_2$ manifold is within the range for three-phonon decay from the $^3P_0$ state, and the initial risetime of the fluorescence, see Fig. 5, was attributed to the decay from the $^3P_0$ level to the $^1D_2$ level. In YLF crystals the $^3P_0$ state decay was mostly radiative and no $^1D_2$ emission was observed after $^3P_0$ excitation.

V. CONCLUSIONS

We have investigated an upconversion process for achieving blue fluorescence induced by one-color IR excitation. The mechanism for upconversion was determined to be a sequential two-photon absorption involving praseodymium ions in the $^1G_4$ state, the first step being far from resonance. The higher efficiency of this upconversion observed in YAG compared to YLF was attributed to a more energetic phonon spectrum which favors the multiphonon absorption involved. From the analysis of the sequential two-photon excitation spectra of YAG:Pr^{3+} and YLF:Pr^{3+}, a number of $^1I_6$ Stark levels, forbidden by the spin-selection rules for one-photon transitions, have been identified. Our recent observation of blue light generation in YAG:Pr^{3+} (Ref. 11) stimulates further studies on upconversion lasing in this material.

ACKNOWLEDGMENTS

One of the authors (M.M.) wishes to thank CNRS organization and Region Rhône-Alpes for supporting him as a visiting scientist. This research has been also funded in part by KBN Grant No. 337069102. The authors wish to thank Dr. R. L. Cone for a critical reading of the manuscript.

[1] A. A. Kaminskii, *Laser Crystals,* 2nd ed. (Springer-Verlag, Berlin, 1990).
[2] J. S. Chivian, W. E. Case, and D. D. Eden, Appl. Phys. Lett. **35**, 124 (1979).
[3] E. G. Gumanskaya, M. V. Korzhik, S. A. Smirnova, V. B. Pavlenko, and A. A. Fedorov, Opt. Spectrosc. (USSR) **72**, 86 (1991).
[4] M. A. Dubinskii, V. V. Semashko, A. K. Naumo, R. Y. Abdulsabirov, and S. L. Korableva, *OSA Proceedings on Advanced Solid State Lasers,* edited by Albert A. Pinto and Tso Yee Fan (Optical Society of America, Washington, DC, 1993), Vol. 15, pp. 195–198.
[5] J. Ganem, W. M. Dennis, and W. M. Yen, J. Lumin. **54**, 79 (1992).
[6] S. K. Gayen, Bin Qing Xie, and Y. M. Cheung, Phys. Rev. B **45**, 20 (1992).
[7] A. Bleckmann, F. Heine, J. P. Meyn, T. Danger, E. Heumann, and G. Huber, *OSA Proceedings on Advanced Solid State Lasers,* edited by Albert A. Pinto and Tso Yee Fan (Optical Society of America, Washington, DC, 1993), Vol. 15, pp. 199–201.
[8] M. E. Koch, A. W. Kueny, and W. E. Case, Appl. Phys. Lett. **56**, 1083 (1990).
[9] B. J. Ainslie, S. P. Craig, and S. T. Davey, J. Lightwave Technol. **6**, 287 (1988).
[10] L. Esterowitz, F. J. Bartoli, R. E. Allen, D. E. Wortman, C. A. Morrison, and R. P. Leavit, Phys. Rev. B **19**, 6422 (1979).
[11] M. Malinowski, M. F. Joubert, and B. Jacquier, Phys. Status Solidi A **140**, K49 (1993).
[12] R. G. Smart, D. C. Hanna, A. C. Tropper, S. T. Davey, S. F. Carter, and D. Szebesta, Electronic Lett. **127**, 1307 (1991).
[13] J. Y. Allain, M. Monerie, and H. Poignant, Electronics Lett. **27**, 1156 (1991).
[14] J. S. Chivian, W. E. Case, and D. D. Eden, Appl. Phys. Lett. **35**, 124 (1979).
[15] D. J. Zalucha, J. C. Wright, and F. K. Fong, J. Chem. Phys. **59**, 997 (1973).
[16] A. Lezama, Phys. Rev. B **34**, 8850 (1986).
[17] E. Antic-Fidancev, M. Lemaitre-Blaise, P. Caro, and J. C. Krupa, Inorg. Chim. Acta **139**, 281 (1987).
[18] J. B. Gruber, M. E. Hills, R. M. Macfarlane, C. A. Morrison, and G. A. Turner, Chem. Phys. **134**, 241 (1989).
[19] M. Malinowski, P. Szczepanski, W. Wolinski, R. Wolski, and Z. Frukacz, J. Phys. Condens. Matter **5**, 6469 (1993).
[20] H. H. Caspers and H. E. Rast, J. Lumin. **10**, 347 (1975).
[21] T. R. Bader and A. Gold, Phys. Rev. **171**, 997 (1968).
[22] M. Galczynski, M. Blazej, and W. Strek, Mater. Chem. Phys. **31**, 175 (1992).
[23] C. de Mello Donegà, A. Meijerink, and G. Blasse, J. Phys. Condens. Matter **4**, 8889 (1992).
[24] F. N. Hooge, J. Chem. Phys. **45**, 4504 (1966).
[25] R. S. Quimby and B. Zheng, Appl. Phys. Lett. **60**, 1055 (1992).
[26] M. Malinowski, R. Wolski, and W. Wolinski, Solid State Commun. **74**, 17 (1990).
[27] R. C. Powell (unpublished).
[28] S. A. Miller, H. E. Rast, and H. H. Caspers, J. Chem. Phys. **52**, 4172 (1970).
[29] C. Garapon, M. Malinowski, M. F. Joubert, A. A. Kaminskii, and B. Jacquier, J. Phys. IV (France) **4**, C4-349 (1994).